

Sensitivity of CAM5-Simulated Arctic Clouds and Radiation to Ice Nucleation Parameterization

SHAOCHENG XIE

Lawrence Livermore National Laboratory, Livermore, California

XIAOHONG LIU

Pacific Northwest National Laboratory, Richland, Washington

CHUANFENG ZHAO AND YUYING ZHANG

Lawrence Livermore National Laboratory, Livermore, California

(Manuscript received 28 July 2012, in final form 18 February 2013)

ABSTRACT

Sensitivity of Arctic clouds and radiation in the Community Atmospheric Model, version 5, to the ice nucleation process is examined by testing a new physically based ice nucleation scheme that links the variation of ice nuclei (IN) number concentration to aerosol properties. The default scheme parameterizes the IN concentration simply as a function of ice supersaturation. The new scheme leads to a significant reduction in simulated IN concentration at all latitudes while changes in cloud amounts and properties are mainly seen at high- and midlatitude storm tracks. In the Arctic, there is a considerable increase in midlevel clouds and a decrease in low-level clouds, which result from the complex interaction among the cloud microphysics, microphysics, and large-scale environment. The smaller IN concentrations result in an increase in liquid water path and a decrease in ice water path caused by the slowdown of the Bergeron–Findeisen process in mixed-phase clouds. Overall, there is an increase in the optical depth of Arctic clouds, which leads to a stronger cloud radiative forcing (net cooling) at the top of the atmosphere. The comparison with satellite data shows that the new scheme slightly improves low-level cloud simulations over most of the Arctic but produces too many midlevel clouds. Considerable improvements are seen in the simulated low-level clouds and their properties when compared with Arctic ground-based measurements. Issues with the observations and the model–observation comparison in the Arctic region are discussed.

AU1

1. Introduction

Climate models exhibit larger intermodel differences in projected Arctic climate change than in other regions (Walsh et al. 2002; Hassol 2004; Vavrus et al. 2009). The spread in Arctic climate change projections is related to differences in model physics, such as in representing Arctic clouds and their microphysical properties, as well as internal variability (Kay et al. 2011a). Arctic clouds strongly influence the earth's radiation budget and their impact on shortwave feedbacks is important for climate feedbacks in climate models (Winton 2006; Kay et al.

2012a). One important cloud microphysical process that has a large impact on model-simulated Arctic clouds is the ice nucleation process (Liu et al. 2007a,b; Xie et al. 2008; Gettelman et al. 2010; Morrison et al. 2012). This is because ice nuclei (IN) play an important role in the glaciation of mixed-phase clouds, which dominate low-level Arctic clouds especially during cold seasons. They also influence ice crystal concentrations in cirrus clouds by competing with homogeneous freezing processes below about -36°C (Karcher and Lohmann 2003; Liu et al. 2012a). Once ice is formed, ice growth from these preexisting ice particles could be accelerated through other important cloud microphysical processes, such as the Bergeron–Findeisen process, for ice crystals to grow at the expense of liquid water (Bergeron 1935; Findeisen 1938). Therefore, the presence of IN can largely influence ice growth and the complex interaction between

Corresponding author address: Shaocheng Xie, Atmospheric, Earth, and Energy Division (L-103), Lawrence Livermore National Laboratory, P.O. Box 808, Livermore, CA 94550.
E-mail: xie2@llnl.gov

the ice and liquid phases of cloud condensate, which in turn affects the radiative properties and lifetime of cold clouds (Phillips et al. 2005; Ekman et al. 2007; Zeng et al. 2009).

Although the importance of ice formation to clouds and their properties is generally accepted, the treatment of IN concentrations in current climate models is still crude because of our poor understanding of the complex ice-formation processes and a general lack of observations of cold clouds. Most existing ice nucleation schemes are developed based on very limited field studies (most conducted at middle and low latitudes) and optimized specifically for where these measurements were observed. They are usually parameterized as a function of temperature and/or ice supersaturation while ignoring IN temporal and spatial variability as a function of aerosol properties. The IN are generally insoluble aerosol particles such as mineral dusts, soot, or black carbon, as well as some biological materials (e.g., Levin and Yankofsky 1983; Diehl et al. 2001; Gorbunov et al. 2001). One example of such simplified ice nucleation schemes is the widely used empirical formulation developed by Meyers et al. (1992, hereafter M1992) for the combined effects of deposition and condensation-freezing nucleation. In M1992, the IN predicted through deposition and condensation freezing is parameterized as a function of ice supersaturation based on measurements at northern midlatitudes and may be applied over the temperature range from -7° to -20°C , ice supersaturation range from 2% to 25%, and water supersaturation range from -5% to 4.5%.

Based on in situ data measured by continuous-flow diffusion-chamber (CFDC) measurements from nine field campaigns conducted in the past 14 yr over many regions of the globe, DeMott et al. (2010, hereafter DM2010) showed a large variability in IN observations in time, space, and temperature. As demonstrated in DM2010, the variability in IN concentration at any temperature encompassed three orders of magnitude while earlier schemes often best fit to the specific data used and have large disagreements with the compiled dataset based on the nine field campaigns. Previous studies (e.g., Bigg 1996) also indicated that Arctic IN concentrations are usually lower than those observed at lower latitudes. This is further confirmed by one recent field campaign in the Arctic, the Mixed-Phase Arctic Cloud Experiment (M-PACE), which was conducted by the U.S. Department of Energy (DOE) Atmospheric Radiation Measurement (ARM) program during the fall season with the relatively clean environment at its Barrow site (Verlinde et al. 2007). By analyzing IN data from M-PACE, Prenni et al. (2007) found that the M1992 parameterization is not representative of average IN behavior encountered

during M-PACE flights. To best fit M-PACE observations of IN, a modified M1992 parameterization was proposed by Prenni et al. (2007), which results in a much smaller ice number density of 0.29L^{-1} relative to 3.23L^{-1} from the original M1992 scheme for a typical temperature range (from -5° to -20°C) of M-PACE clouds. In a sensitivity study with the Geophysical Fluid Dynamics Laboratory (GFDL) Global Atmospheric Model, version 2 (AM2), Xie et al. (2008) showed that the use of the modified M1992 parameterization by Prenni et al. (2007) led to a significant increase in both cloud fraction and cloud liquid water path for the period where single-layer low-level mixed-phase clouds were observed during M-PACE.

To improve ice crystal number concentrations predicted in climate models, more physically based ice nucleation schemes were developed in recent years. For example, Phillips et al. (2008) introduced an ice nucleation parameterization that links the variation of IN concentrations to aerosol properties such as aerosol surface area densities of several aerosol species (mineral dust, black carbon, and hydrophobic organics), relative humidity, and temperature. Similarly, DM2010 showed that IN concentrations can be associated with the temperature and concentration of aerosol particles (e.g., mineral dust) larger than $0.5\ \mu\text{m}$ in diameter based on a larger dataset as mentioned earlier. Based on cloud chamber experiments, Niemand et al. (2012) presented a particle-surface-area-based parameterization for the immersion freezing on desert dust particles in the temperature range from -12° to -36°C . These parameterizations were basically fittings of observed IN as a function of ambient conditions and concurrent aerosol properties. Different from these empirical parameterizations, Chen et al. (2008) used a statistical model that parameterizes the rate of heterogeneous ice nucleation as a function of temperature and ice supersaturation, as well as properties of IN such as size, contact angle of ice germ on the substrate, and activation energy. Chen et al. (2008) is based on the theoretical formulation of the classical nucleation theory (CNT) with aerosol-specific parameters constrained from experiments.

In this study, we examine both the M1992 scheme and the DM2010 scheme in the National Center for Atmospheric Research (NCAR)–DOE Community Atmosphere Model, version 5.1 (CAM5.1). For simplicity, we just refer to the model version as CAM5. The goal of this study is to better understand the important role of ice nucleation processes in clouds and radiation simulated by climate models with an emphasis on the Arctic region. Specifically, we would like to know how modeled cloud types and their properties vary with the treatment of ice nucleation processes and how these changes impact

AU2

the earth's radiative budget. Although this is a sensitivity study, both satellite observations and field data are used to as references for model simulations. More details about CAM5, the two tested ice nucleation schemes, numerical experiments, and observational data are described in section 2. Results are discussed in section 3. Summary and discussion are presented in section 4.

2. Model, experimental details, and observations

a. CAM5

AU3 CAM5 is the latest version of the CAM that contains a range of significant enhancements and improvements in the representation of physical processes (P. J. Rasch et al. 2012, personal communication). Almost all of the physical parameterizations in its previous version CAM4 have been changed in CAM5, except for the deep convection scheme, which was originally developed by Zhang and McFarlane (1995) with the dilute convective available potential energy (CAPE) modification described in Neale et al. (2008). For cloud microphysics, a two-moment cloud microphysics scheme for stratiform clouds (Morrison and Gettelman 2008; Gettelman et al. 2010), which features activation of aerosols to form cloud drops and ice crystals and allows ice supersaturation, has been implemented into CAM5 to replace the one-moment cloud microphysics scheme (Rasch and Kristjánsson 1998) used in CAM4. The primary ice crystal nucleation in Gettelman et al. (2010) is based on the scheme developed by Liu et al. (2007a). In this scheme, homogeneous freezing on sulfate aerosol competing with heterogeneous immersion nucleation on mineral dust is the ice nucleation mechanism for ice clouds ($T < -37^\circ\text{C}$). For mixed-phase clouds ($-37^\circ < T < 0^\circ\text{C}$), M1992 is used for deposition/condensation nucleation for temperatures between 0° and -20°C , with a constant IN concentration for $T < -20^\circ\text{C}$. In this sensitivity study, we replace the M1992 scheme by DM2010 to represent the deposition/condensation nucleation processes in CAM5. Note that the DM2010 scheme is applied to the entire temperature range for mixed-phase clouds: that is, $-37^\circ < T < 0^\circ\text{C}$. The aerosol fields used for aerosol–cloud interactions are predicted from the CAM5 modal aerosol module (MAM) (Liu et al. 2012b). In the CAM5 MAM, aerosol size distributions are represented by three lognormal modes: Aitken, accumulation, and coarse modes. Mass mixing ratios of different aerosol species and number concentrations are predicted for each aerosol mode. Dust number concentration in the accumulation with diameters larger than $0.5\ \mu\text{m}$ is calculated from the predicted dust mass mixing ratio in the accumulation mode and the prescribed size distribution

for transported dust (Zender et al. 2003). Dust number concentration in the coarse mode is calculated from the predicted total number concentration in the coarse mode weighted by the mass fraction of dust in the mode. The sum of these two dust number concentration is used in the scheme of DM2010. More details on the aerosol simulations can be found in Liu et al. (2012b).

1) THE M1992 SCHEME

The M1992 scheme was designed for the combined effects of deposition and condensation-freezing nucleation based on data taken from CFDC at northern midlatitudes (Rogers 1982; Al-Naimi and Saunders 1985). As defined in M1992, deposition nucleation is the formation of ice in a supersaturated (with respect to ice) environment. This ice-formation process is assumed to occur for any condition that exceeds ice saturation at freezing temperatures. Condensation-freezing nucleation is the sequence of events whereby a cloud condensation nuclei (CCN) initiates freezing of the condensate. It requires conditions mostly exceeding water supersaturation at freezing temperatures. For these conditions, deposition nucleation may also occur. It is impossible in practice to distinguish the separate contributions of deposition and condensation freezing when a cloud parcel is supersaturated with respect to water without special experiments. To best fit these datasets, the number of pristine ice crystals ($N_{\text{in}}; \text{l}^{-1}$) predicted because of deposition and condensation freezing is parameterized as

$$N_{\text{in}} = e^{\{a+b[100(S_i-1)]\}}, \quad (1)$$

where $S_i - 1$ is the fractional ice supersaturation, $a = -0.639$, and $b = 0.1296$. The square of the correlation coefficient for this fit is 0.82. As shown in Eq. (1), N_{in} is parameterized as a function of ice supersaturation without considering the association of its spatial and temporal variations with aerosol properties. The equation may be strictly applied over the temperature range from -7° to -20°C , ice supersaturation range from 2% to 25%, and water supersaturation range from -5% to 4.5% .

2) THE DM2010 SCHEME

The DM2010 scheme was developed to determine the overall temperature and aerosol particle size dependencies of IN active under mixed-phase cloud conditions based on nine separate field studies conducted over the past 14 yr in many regions of the globe,

$$N_{\text{in},T_K} = a(273.16 - T_K)^b (N_{\text{aer},0.5})^{[c(273.16+T_K)+d]}, \quad (2)$$

where $a = 0.0000594$, $b = 3.33$, $c = 0.0264$, $d = 0.0033$, **AU4** T_K is cloud temperature in kelvins, $N_{\text{aer},0.5}$ is the number

AU5 concentration (scm^{-3}) of aerosol particles with diameters larger than $0.5 \mu\text{m}$, and N_{in,T_K} is IN concentration (l^{-1}) at T_K . Note that sea salt particles are excluded from $N_{\text{aer},0.5}$. Relative to M1992, the unique feature of the DM2010 scheme is to link the variations of IN concentrations to aerosol particles. The correlation coefficients for power law fits to the multistudy dataset are in a range of 0.6–0.8. As discussed in DM2010, their scheme significantly improves the agreement with the integrated dataset from the nine separate field studies where the M1992 scheme largely overestimates the observed IN concentrations (see Fig. 3 in DM2010).

b. Model integrations

The CAM5 with its finite volume dynamic core at the resolution of $0.9^\circ \times 1.25^\circ$ in the horizontal and 30 levels in the vertical is used in this study. In addition, we have included a fix of the inconsistency of cloud macrophysics for cloud condensation and cloud microphysics for droplet activation caused by the time splitting in CAM5 (H. Morrison, NCAR, 2011, personal communication; Liu et al. 2011). Two 11-yr “free running” simulations of CAM5, one with the default M1992 scheme (CAM50) and the other one with the DM2010 scheme (CAM5DM) for ice nucleation, are conducted following the prototype described in the second phase of the Atmospheric Model Intercomparison Project (AMIP II) (Gates et al. 1999) with sea surface temperatures (SST) and sea ice prescribed from the observations. The last 10 yr of data for these two runs are analyzed and compared.

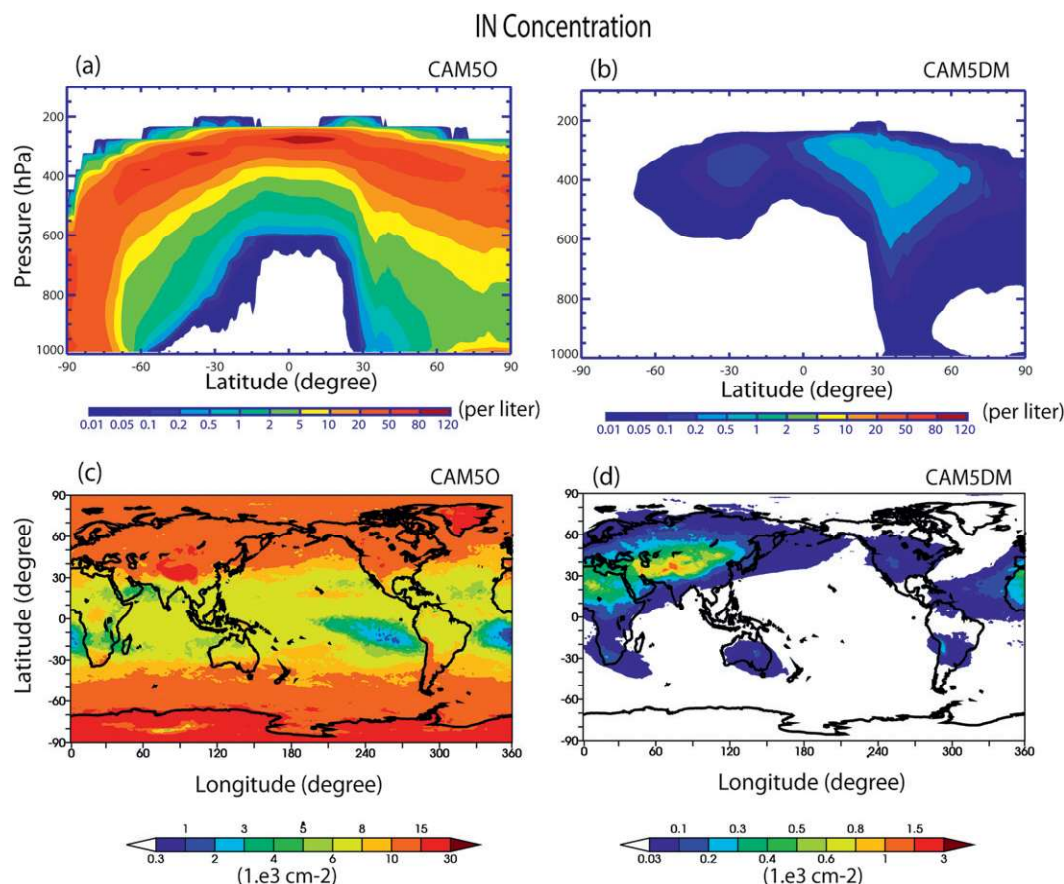
c. Observations

The data used to compare with model simulations include clouds measured from the International Satellite Cloud Climatology Project (ISCCP; Rossow and Schiffer 1999), the Moderate Resolution Imaging Spectroradiometer (MODIS; Platnick et al. 2003), and the *Cloud–Aerosol Lidar and Infrared Pathfinder Satellite Observation* (CALIPSO). Radiation fluxes are from the Clouds and the Earth’s Radiant Energy System (CERES) observations (Wielicki et al. 1996) and the Earth Radiation Budget Experiment (ERBE; Barkstrom 1984). These observations except for CALIPSO are available from the NCAR CAM diagnostic data package (<http://www.cgd.ucar.edu/amp/amwg/diagnostics/>). The CALIPSO data are obtained from the Cloud Feedback Model Intercomparison Project (CFMIP): the General Circulation Model–Oriented Cloud CALIPSO Product (GOCCP) (Chepfer et al. 2010). The CERES data are the Energy **AU6** Balanced and Filled (EBAF) 2.6 product (Loeb et al. 2009), which provides monthly-mean top-of-the-atmosphere (TOA) radiative fluxes. The ISCCP data are from July 1983 to June 2008, the MODIS data are from January

2003 to December 2010, the CALIPSO data are from June 2006 to December 2010, the ERBE data are from February 1985 to April 1989, and the CERES data are from March 2000 to February 2010. To improve the comparison between model clouds and satellite observations, outputs from the CFMIP (Bony et al. 2011) Observation Simulator Package (COSP) (Bodas-Salcedo et al. 2011; Kay et al. 2012b) embedded in CAM5 are used to compare with the corresponding satellite cloud observations. In addition to these satellite data, long-term ground-based cloud and radiation measurements from 1998 to 2010 at Barrow (71.3°N , 156.6°W) from the Atmospheric Radiation Measurement Program (ARM) Best Estimate (ARMBE) dataset (Xie et al. 2010) are also used for the model evaluation.

As discussed in earlier studies (e.g., Kay et al. 2012b; Pincus et al. 2012), large differences can exist among these satellite observations because of different instrument limitations and differences in the algorithms used to retrieve cloud properties. For example, there are considerable differences in cloud frequency between ISCCP and MODIS retrieved cloud types, particularly for high- and mid-top thin clouds, where the MODIS value is much smaller than the ISCCP value. This is mainly because of significant differences in the algorithms used to retrieve cloud-top pressure from these two datasets (Pincus et al. 2012). In addition, ISCCP can overestimate middle-top clouds when compared with MODIS under the situation that optically thin cirrus overlay low-top clouds. It should be noted that both ISCCP and MODIS use passive instruments and their interpretations of cloud measurements rely on albedo and thermal contrast between the clouds and the underlying surface. This can lead to large uncertainty in their retrieved cloud data in the Arctic region during the cold months when snow is present. In the Arctic, the active instrument CALIPSO probably provides the most reliable cloud observations because of its capability in detecting optically thin clouds and its retrieval that does not rely on albedo or thermal contrast (Kay et al. 2012a; Barton et al. 2012).

Differences are also found in radiative fluxes between CERES and ERBE, which are largely from the algorithms used to convert radiances into fluxes. The ERBE uses angular directional models (AMD) for the conversion, which have only four cloud amount classifications, while CERES uses surface type, cloud amount, phase, and optical depth for shortwave (SW) radiation and precipitable water, lapse rate, and emissivity for long-wave (LW) radiation. Besides, the significant sea ice loss and warming in recent years in the Arctic region can also contribute to the differences between these two datasets. More discussion on these differences as well as on potential issues with ground-based measurements will



AU11 FIG. 1. IN concentrations produced by (left) CAM50 and (right) CAM5DM: (a),(b) zonal and annual mean and (c),(d) vertically integrated annual mean.

be given in next section, where these data are used in model evaluations.

3. Results

a. Impact on annual-mean clouds and cloud properties over the globe

F1 Figures 1a–d compare IN concentrations in mixed-phase clouds simulated by CAM50 and CAM5DM. Consistent with previous studies (Prenni et al. 2007; DM2010), the IN concentrations produced by CAM50 are significantly larger (up to two orders of magnitude) than those predicted by CAM5DM at all latitudes. The IN concentrations increase with height and latitude in CAM50 with three maxima seen in the upper troposphere (400–300 hPa) associated with the ascending branches of the Hadley cell and the midlatitude cell (Fig. 1a). The IN concentrations are much higher at the middle and high latitudes than in the tropics (Fig. 1c). In contrast, the IN concentrations in CAM5DM are mainly located at northern midlatitude lands where there are

large aerosol particles (mineral dusts) over the Sahara desert and Asian deserts (Figs. 1b,d). The lack of IN concentrations in the Antarctic region in CAM5DM is because of the lack of dust particles.

The change of the IN concentrations has a large impact on cloud water contents in the mixed-phase clouds. As shown in Figs. 2a,b, considerable differences are noticed in the annual-mean liquid water path (LWP) and ice water path (IWP) simulated with these two schemes particularly at high latitudes and the midlatitude storm track regions. Over these regions, the smaller IN concentrations simulated by CAM5DM result in an increase ($>10 \text{ g m}^{-2}$) of LWP and a decrease ($>3 \text{ g m}^{-2}$) of IWP. This is has been shown to be caused by the slowdown of the Bergeron–Findeisen process in mixed-phase clouds, which results in a smaller conversion rate from cloud liquid to ice/snow based on the process analysis (Liu et al. 2007b; Xie et al. 2008; Liu et al. 2011).

Similar to LWP and IWP, the largest impact on clouds is also at high latitudes and midlatitude storm tracks, where there is a significant increase in midlevel clouds (Fig. 3b) and a large decrease in low-level clouds (Fig. 3c)

F2

F3

Difference in Cloud Properties (CAM5DM - CAM50)

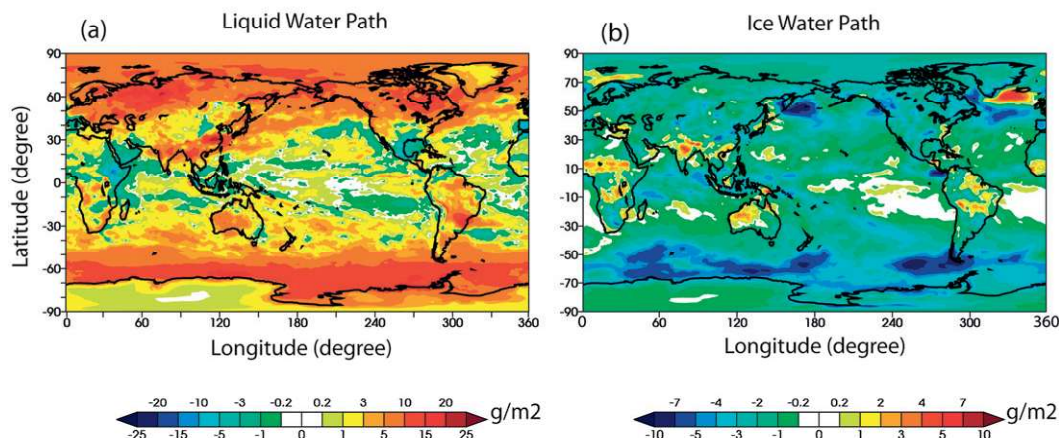


FIG. 2. Differences between CAM5DM and CAM50 in annual-mean (a) LWP and (b) IWP.

with the use of the DM2010 scheme. Changes in high-level clouds (Fig. 3a) are moderate with a general increase of cloud amount seen over most regions. As a result, the changes in total clouds (Fig. 3d) are relatively small. In the tropics, moderate changes are seen only in some regions for mid- and high-level clouds. For example, there is a noticeable reduction in midlevel clouds over the tropical Indian Ocean, intertropical convergence zone (ITCZ), and South Pacific convergence zone (SPCZ). This is because the change of ice number concentrations mainly affects mixed-phase clouds, which occur more often at higher latitudes than in the tropics.

Directly linking the changes in cloud amount to the changes in IN concentrations is difficult in CAM5 because its cloud fraction and cloud water contents are determined by separate equations (P. J. Rasch et al. 2012, personal communication). In CAM5, cloud fraction is diagnosed primarily based on grid-mean relative humidity (RH) (and convective updraft mass fluxes for cumulus clouds). This is indicated by the strong correlation between changes in mid- and high-level cloud amount (Figs. 3a,b) and changes in mid- and upper-tropospheric RH (Figs. 4a,b). The large increase of midlevel clouds is the result of the large increase of midlevel RH.

However, the strong dependency on RH is not seen for low-level clouds (Figs. 3c, 4c), which seem more related to lower-tropospheric stability (LTS) (Fig. 4d). Here, the LTS is defined as the difference in potential temperature at the model level of 691 hPa and the lowest model level of 993 hPa. It is seen that the large decrease of low-level cloud amount corresponds well with the large decrease of LTS at high latitudes. The strong relationship between low-level clouds and LTS was found

from both observational (e.g., Klein and Hartmann 1993) and modeling studies (e.g., Zhang et al. 2009; Kay et al. 2011b; Barton et al. 2012). It should be noted that the stratocumulus parameterizations based on LTS developed by Klein and Hartmann (1993), which were used in earlier versions of CAM, are no longer used in CAM5. Nevertheless, LTS seems to still largely influence CAM5 low-level cloud simulations probably through changing boundary layer structures. This warrants further investigation through detailed process-level studies. The above results suggest that the changes in cloud amount are the result of complex interactions among cloud macrophysics, microphysics, and the large-scale environment.

b. Important effect on Arctic clouds and radiation

The preceding results indicate that Arctic clouds have the largest sensitivity to ice nucleation parameterizations, and therefore we will emphasize our analysis on the Arctic region (60°–80°N) in the following discussion. Beyond 80°N, there is generally a lack of satellite data, especially during the winter months. Note that this selection may leave out stronger signals of the impacts with the change of ice nucleation scheme as indicated in Figs. 2 and 3.

Figure 5 compares the annual-mean model-simulated Arctic clouds with CALIPSO observations. The mean errors and root-mean-square (RMS) errors are shown at the top right of the panels. The model clouds are from the CALIPSO simulator output. As discussed earlier, the active CALIPSO instrument provides probably the most reliable satellite measurements of clouds in the Arctic region. In general, the CAM50 overproduces the Arctic clouds at all altitudes with the largest biases

F4

F5

Difference in Clouds (CAM5DM - CAM50)

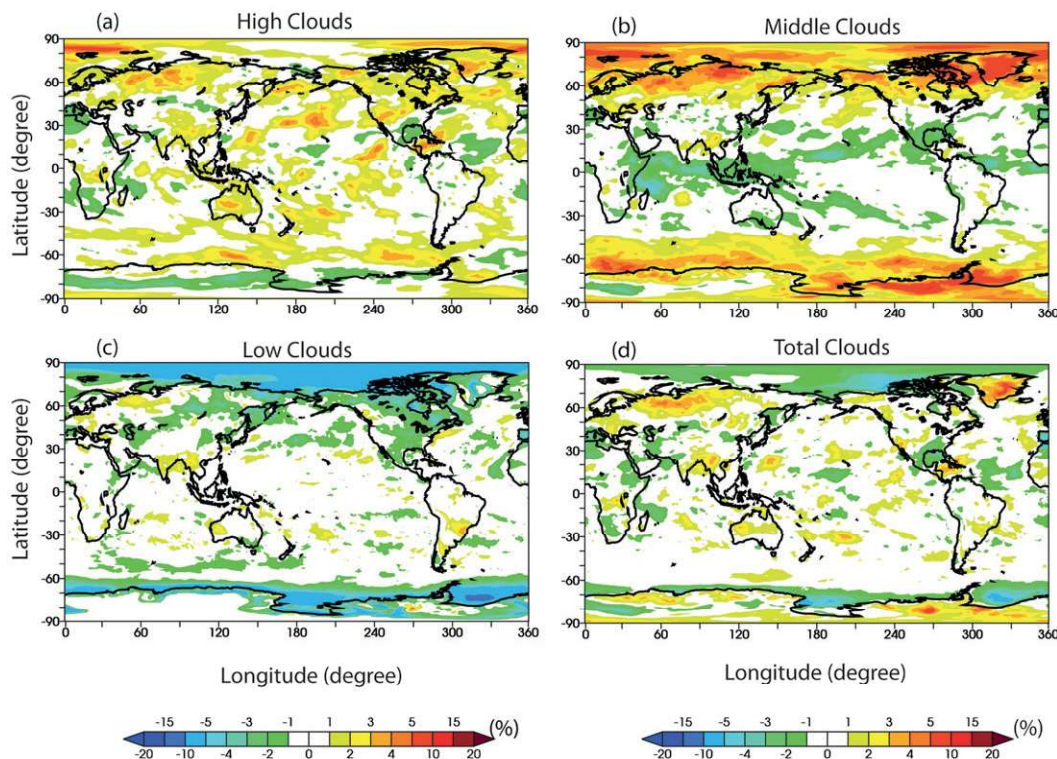


FIG. 3. Differences between CAM5DM and CAM50 in annual-mean (a) high-level, (b) midlevel, (c) low-level, and (d) total clouds.

seen in low-level clouds as indicated by both mean and RMS errors (Figs. 5a,c,e). Consistent with Fig. 3, CAM5DM produces more midlevel clouds over almost the entire Arctic in comparison with CAM50 (Fig. 5d), indicating that the bias in midlevel clouds shown in Fig. 5c is exaggerated. The low-level clouds simulated by CAM5DM are fewer than CAM50 over most of the Arctic (Fig. 5f); however, the mean value is almost unchanged for these two runs. This is inconsistent with Fig. 3c, where low-level clouds are considerably reduced in CAM5DM. The inconsistency is caused by the fact that the clouds from satellite simulator output are only those clouds that the corresponding satellite sees, while the clouds produced by the models contain all types of clouds. For high-level clouds, the result is also mixed. A relatively large increase of high-level clouds is seen over Greenland and its nearby seas and over northern Russia, while a considerable reduction of cloud amounts is found in the Kara Sea, Barents Sea, Canada Basin, North Pacific Ocean, and Sea of Okhotsk (Fig. 5b). It is interesting to note that the regions with the largest decrease of high-level cloud amounts (e.g., in the Kara Sea and Barents Sea) correspond well with those where CAM50 has the

largest overestimation of high-level clouds. This indicates the improved high-level cloud simulation over these regions with the new ice nucleation scheme. It should be noted that the color scale in Fig. 5 is different for the left and right panels. The differences in cloud amount between these two models (right panels), as shown in both mean and RMS errors, are much smaller than those between CAM50 and CALIPSO (left panels), indicating that the changes in cloud amount particularly in low- and high-level cloud amounts are minor relative to the model errors.

Figure 6 shows the cloud frequencies averaged over March–September from 60° to 80°N for the nine ISCCP cloud types in ISCCP and the ISCCP simulator in CAM50 and CAM5DM. Only daytime data are used in obtaining the means because cloud optical thicknesses from ISCCP are determined from visible radiance measurements. We also exclude the boreal winter months in the Arctic region for the same reason. We first examine how sensitive the simulated cloud types are to the change of IN concentrations caused by the two ice nucleation schemes. This is the main purpose of this study. Consistent with earlier discussions, lower IN concentrations in

F6

Difference in RH and LTS (CAM5DM - CAM50)

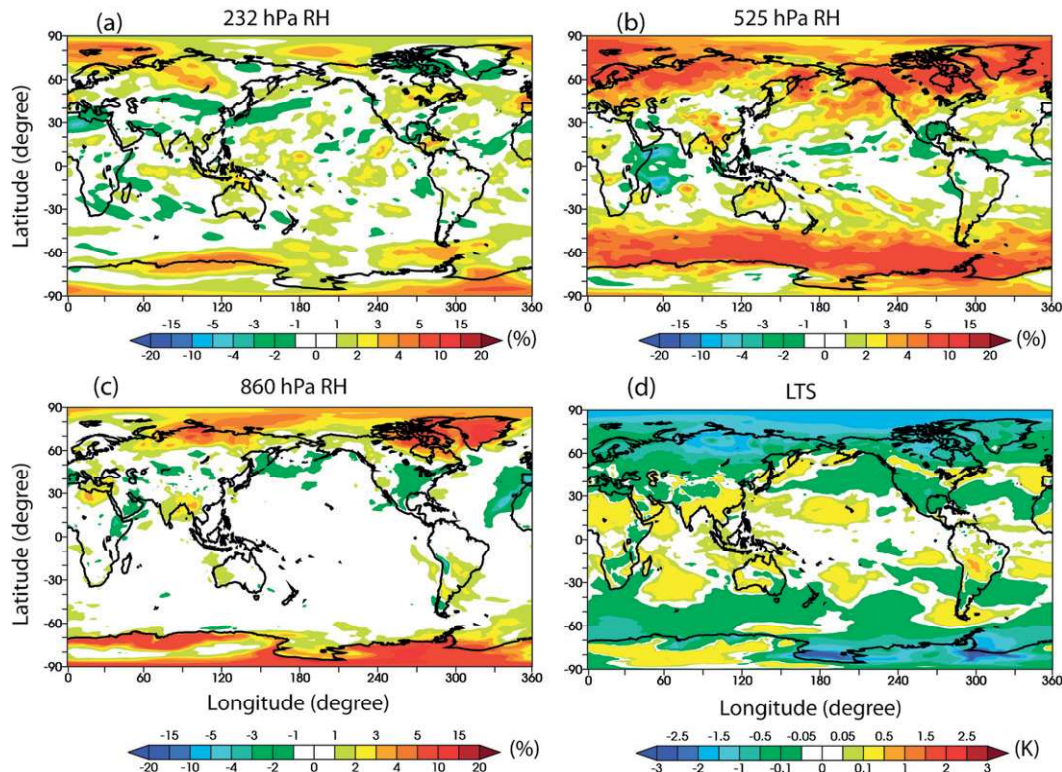


FIG. 4. Differences between CAM5DM and CAM50 in annual-mean RH at (a) 232, (b) 525, and (c) 860 hPa and (d) LTP.

CAM5DM lead to a clear increase in middle-top clouds, particularly for optically intermediate and thick clouds where there is a roughly 30%–40% increase relative to those produced by CAM50. For high- and low-top clouds, however, the results are mixed. The CAM5DM generates fewer optically thin and intermediate high-top clouds and optically thin low-top clouds while it simulates more optically thick high-level clouds and optically intermediate and thick low-top clouds.

F7 Similar results are seen in Fig. 7, which displays results from MODIS and the MODIS simulator, even though the magnitude of these changes in cloud types is slightly different from ISCCP. The only inconsistency between the two simulator outputs is in optically thin middle-top clouds for which CAM5DM has more ISCCP type of thin middle-top clouds than CAM50 while the opposite result is seen from the MODIS simulator output. Overall, the smaller IN concentrations in CAM5DM result in an increase of cloud optical depth τ of Arctic clouds and therefore clouds are much brighter than those in CAM50. This has a large impact on the radiative budget in the Arctic region, as we will discuss later. It is noticed that there is an overall decrease of high-top cloud amount

in CAM5DM relative to CAM50, as shown in Figs. 6 and 7. This is also inconsistent with the increase in high-level clouds in CAM5DM seen in fig3 and 5. In addition to the difference in viewing clouds between satellite and climate models as discussed earlier, this is also partially because Figs. 6 and 7 only use daytime data from March to September while Figs. 3 and 5 are annual means that include both seasonal and diurnal variability.

We now compare these model results with the ISCCP and MODIS observations shown in Figs. 6 and 7. There are large differences between the two satellite datasets, specifically for high- and middle-top thin clouds, where MODIS is about 20% of the ISCCP value. As indicated earlier, this is mainly because of considerable differences in the algorithms used to retrieve cloud-top pressure in these two datasets. Despite these differences between these two datasets, it appears that CAM5DM slightly improves the model simulation of optically thin low-top clouds while it exaggerates the problem that the model produces too many optically thick middle- and high-top clouds relative to both the ISCCP and MODIS observations.

Difference in Clouds

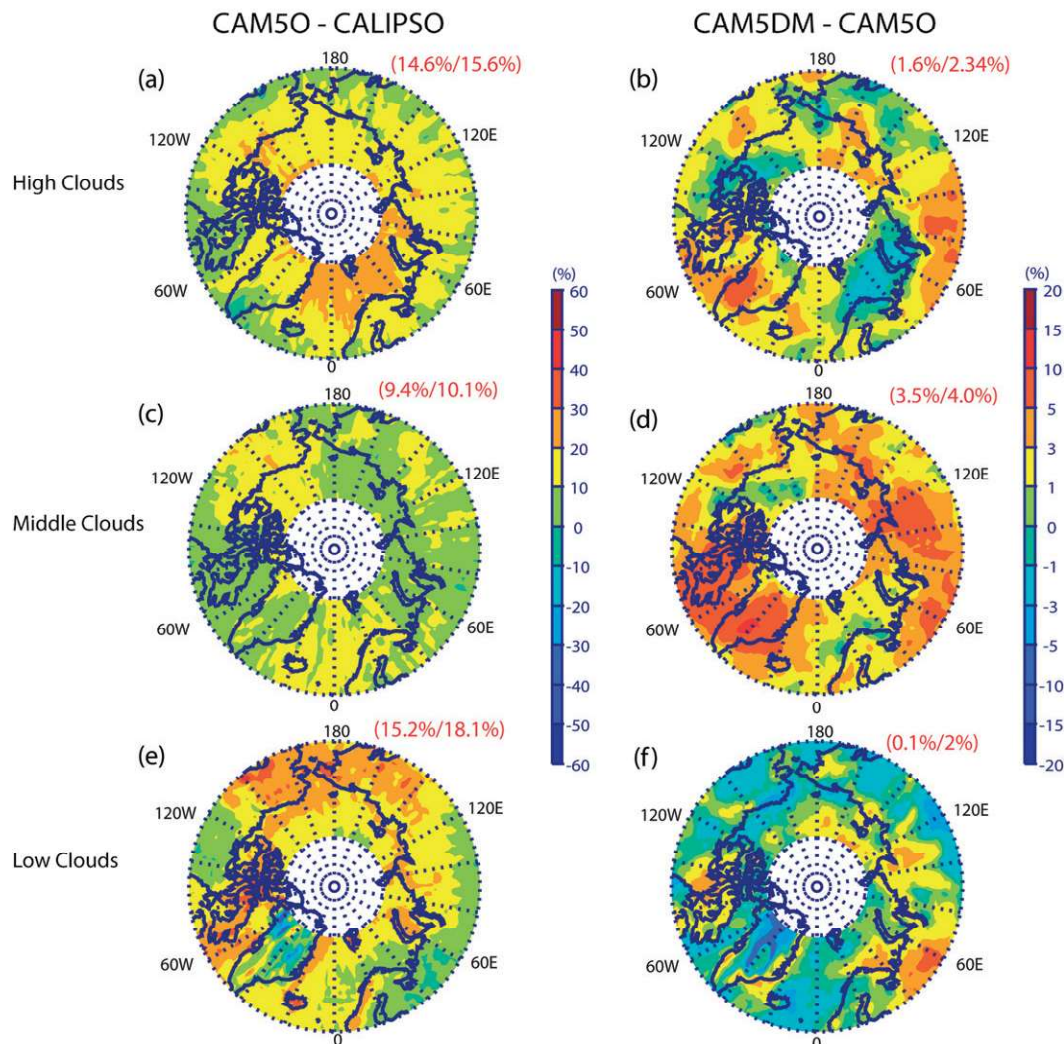


FIG. 5. Differences in annual-mean (a),(b) high-level, (c),(d) midlevel, and (e),(f) low-level clouds between CAM5O and CALIPSO (left) and between CAM5DM and CAM5O (right). The color scale for (left) and (right) is different. The mean errors/RMS errors are shown in red at the top right of the panels.

We next examine the collective impact of the change of cloud types on cloud radiative forcing (CRF) at the TOA. The CRF is calculated by taking the difference between clear-sky and all-sky radiative fluxes. Similarly, Fig. 8 shows the mean cloud radiative forcing at the TOA averaged from March to September and between 60° and 80°N from the ERBE and CERES observations and from the two model simulations. In comparison with CAM5O, CAM5DM has a stronger LW, SW, and net cloud radiative forcing (cooling) at the TOA. The differences are about 1.4 and -3.9 W m^{-2} for the LW and SW CRF, respectively, which results in -2.5 W m^{-2} in net CRF cooling (Fig. 8d). This is consistent with the fact that clouds are brighter in CAM5DM than CAM5O

as discussed earlier. The stronger CRF produced by CAM5DM is seen over the entire Arctic region with considerable spatial variability (Fig. 9).

We note that the differences shown in the TOA CRF between CAM5O and CAM5DM are well within the uncertainty in the observations, which can be roughly represented by the differences between the two satellite observations. As shown in Fig. 8, CERES shows a similar LW CRF but 6.8 W m^{-2} smaller SW CRF than ERBE. This leads to a smaller net CRF (by 8 W m^{-2}) in CERES than the ERBE value in this region. Again, the differences in these two satellite datasets are largely caused by the algorithms used to convert radiances into fluxes as discussed in section 2c. Reducing

F9

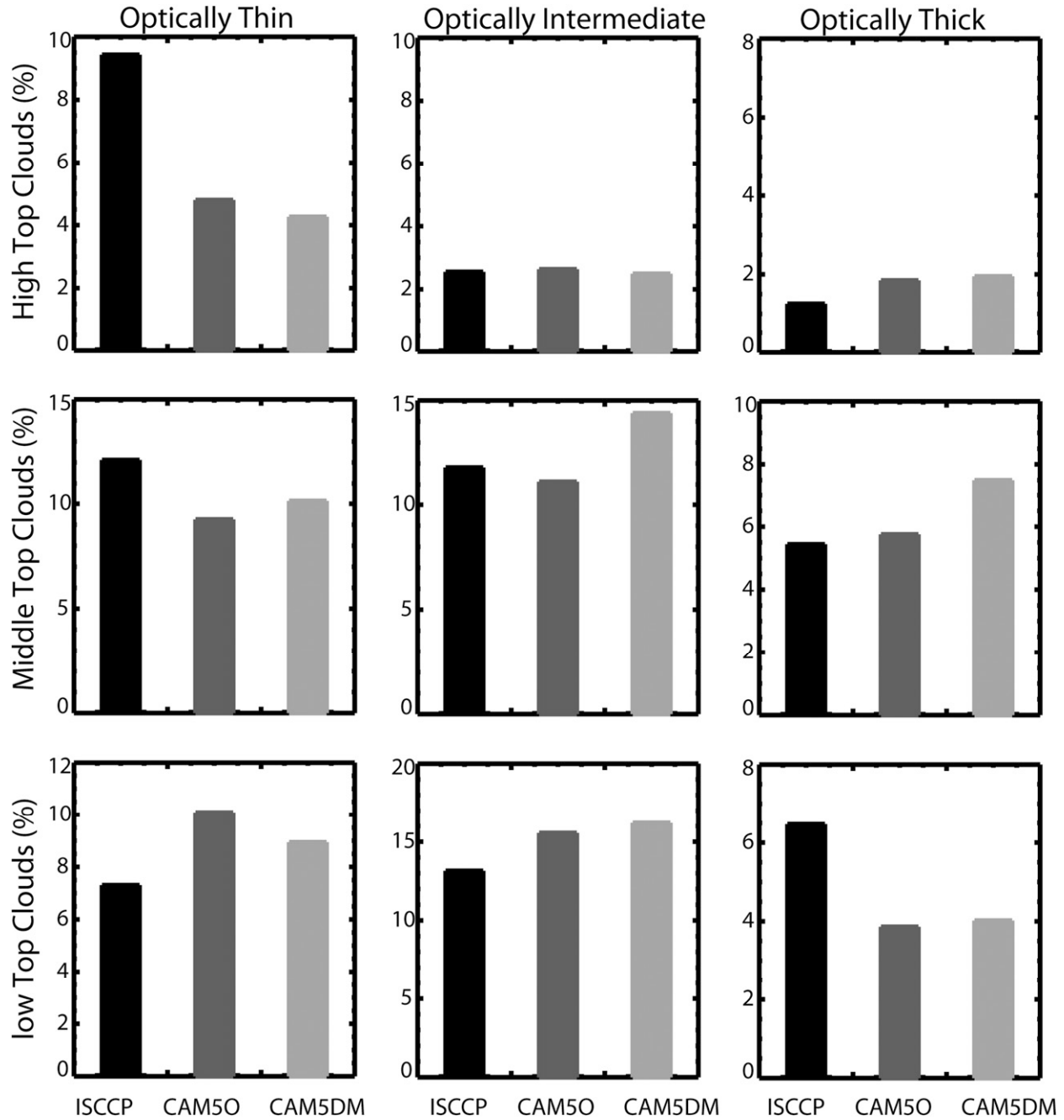


FIG. 6. The cloud frequency for the nine ISCCP cloud types in ISCCP and the ISCCP simulator in CAM5DM and CAM50 averaged over March–September for the Arctic region (60°–80°N). The high-, middle-, and low-top clouds are defined as those with cloud-top pressure less than 440 hPa, between 680 and 440 hPa, and larger than 680 hPa, respectively. The optically thin, intermediate, and thick clouds are defined as those with the cloud optical depth in the ranges of 0.02–3.6, 3.6–23, and larger than 23, respectively.

the uncertainty can help better assess the model performance.

c. Comparison with ground-based observations

In this section, we perform a further evaluation of the performance of these two ice nucleation schemes in

simulating Arctic clouds and radiation with the decade-long ARM measurements at its Barrow site (71.3°N, 156.6°W). Specifically, we use the ARMBE dataset, which is an hourly dataset that assembles cloud and radiation measurements from relevant ARM value-added products with stringent quality controls applied to remove

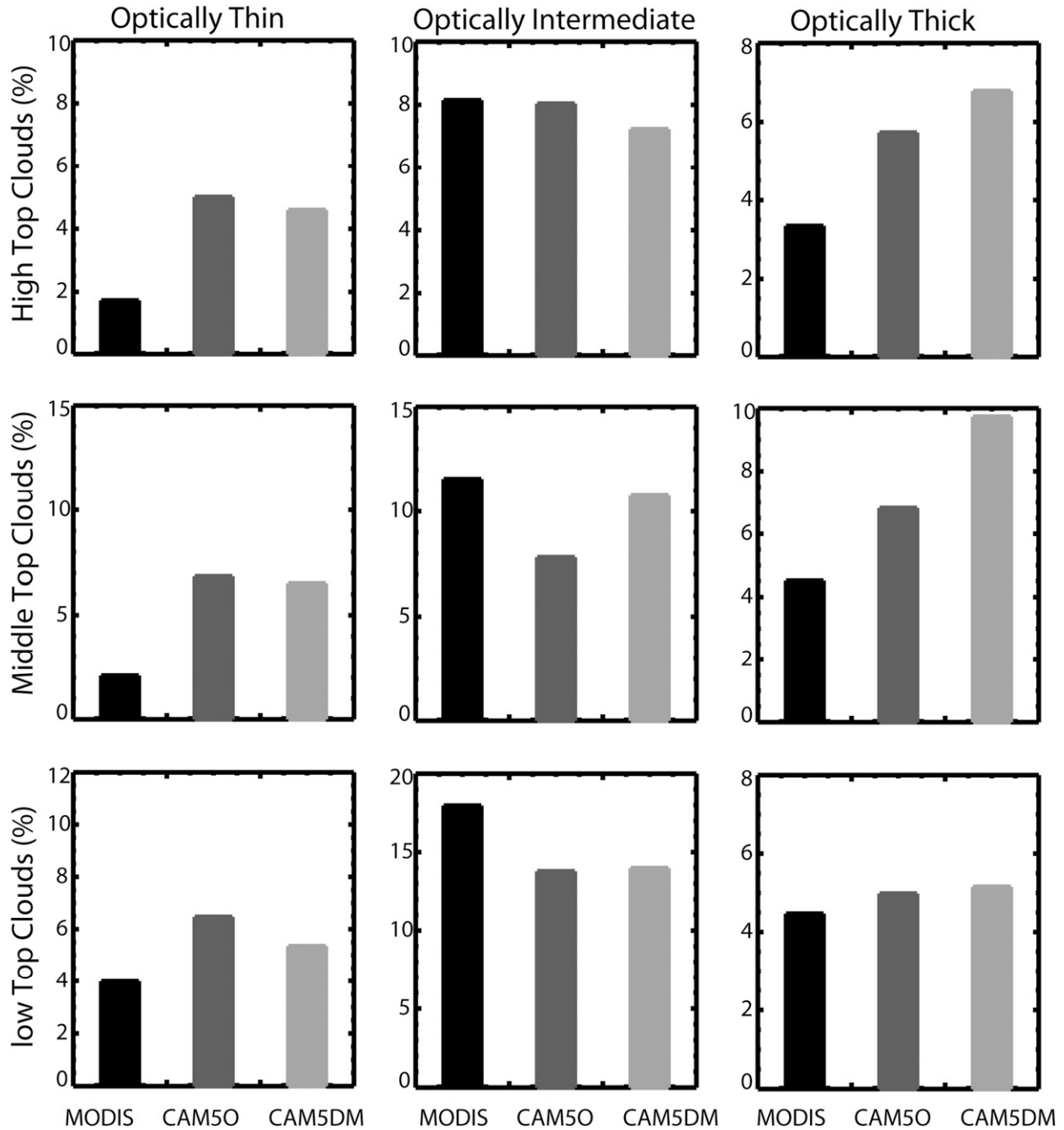


FIG. 7. As in Fig. 6, but for the cloud frequency in MODIS and the MODIS simulator in CAM5 and CAM5DM.

suspicious data points (Xie et al. 2010). Model results at a model grid point that is closest to the ARM Barrow site are compared with the ARM observations. The location of the selected model grid point is (71.15°N, 156.25°W), which represents an area of 110 km × 35 km. One common problem with using ground-based data in climate model evaluations is that the observations are often available at a limited number of stations and they

may not be representative of an area that a typical current climate model grid box represents. This is particularly true for the ARM Barrow site, which is coastal. As a result, the corresponding CAM grid cell for ARM Barrow is a mix of land and ocean. This issue should be borne in mind when interpreting model–observation comparison results.

Figures 10a–c show the time–pressure cross section of observed and simulated monthly-mean cloud fraction at

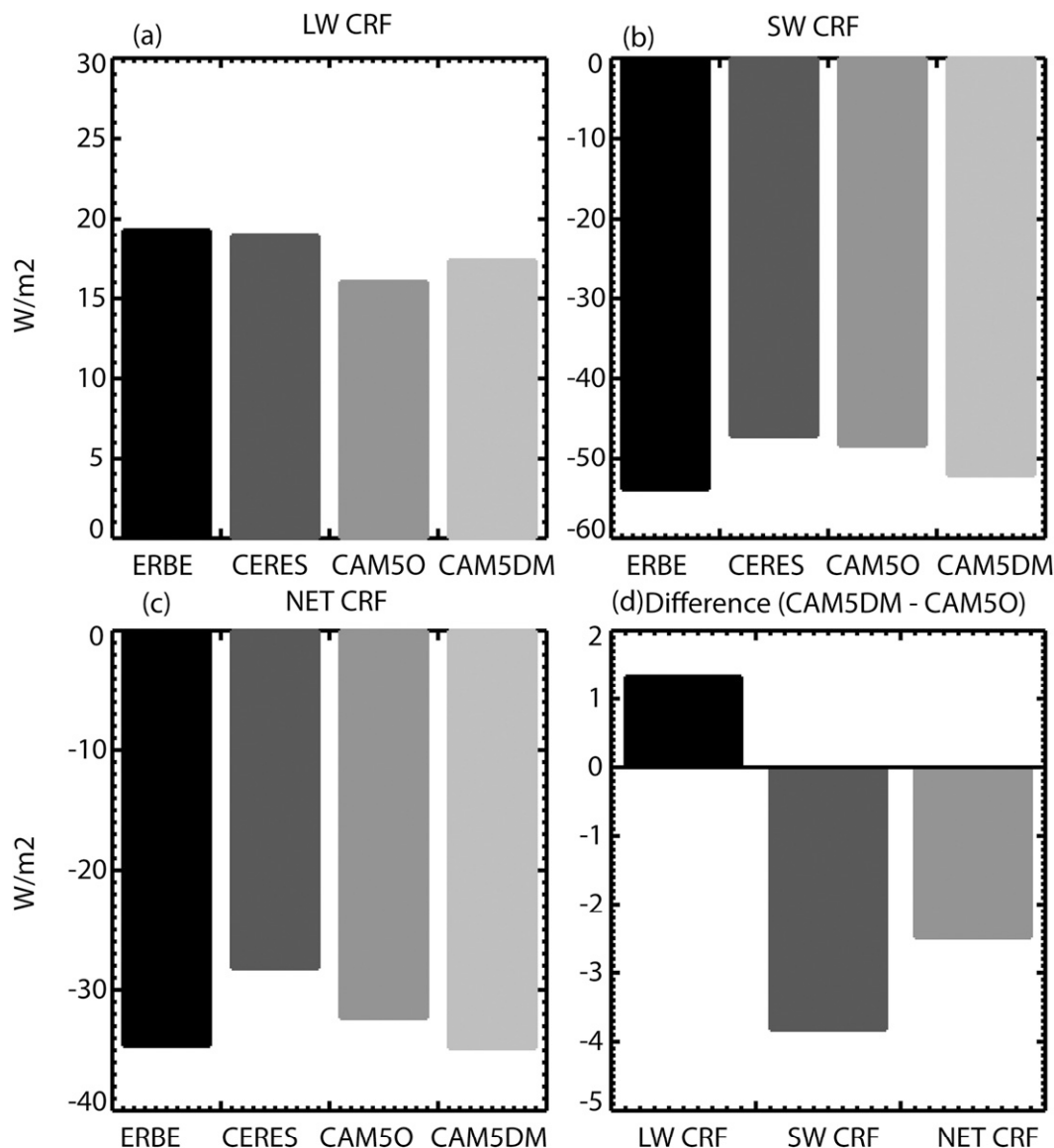


FIG. 8. The CRF at the TOA averaged over March–September for the Arctic region (60°–80°N) from measurements and models. For (a) LW CRF; (b) SW CRF; (c) net CRF; and (d) differences in LW, SW, and net CRF between CAM5DM and CAM5O.

Barrow from ARM, CAM5O, and CAM5DM, respectively. Their seasonal-mean vertical profiles for spring [March–May (MAM)], summer [June–August (JJA)], fall [September–November (SON)], and winter [December–February (DJF)] are displayed in Fig. 11. The observations are based on 13-yr ARM cloud measurements from 1998 to 2010 by integrating measurements from the ARM cloud radar and other sensors using the active remotely sensed clouds locations (ARSCL) algorithm (Clothiaux et al. 2000). One issue with the ARSCL clouds is that cloud radar tends to underestimate the cloud-top heights for high-altitude clouds because it is unable to detect

cloud particles that are too small. One way to address this issue is to developing and implementing a ground-based cloud radar simulator in climate models as it has been done for satellites (i.e., COSP). Without using a cloud radar simulator, it will be difficult to quantitatively evaluate model performance with ground-based cloud radar measurements. Another issue is that cloud radar–detected cloud base can be contaminated with ice precipitation. To reduce this problem, we use the ARM laser ceilometers and micropulse lidar measurements, which are usually insensitive to ice precipitation or clutter, to determine the cloud base (Xie et al. 2010). As

Difference in Cloud Radiative Forcing (CAM5DM - CAM50)

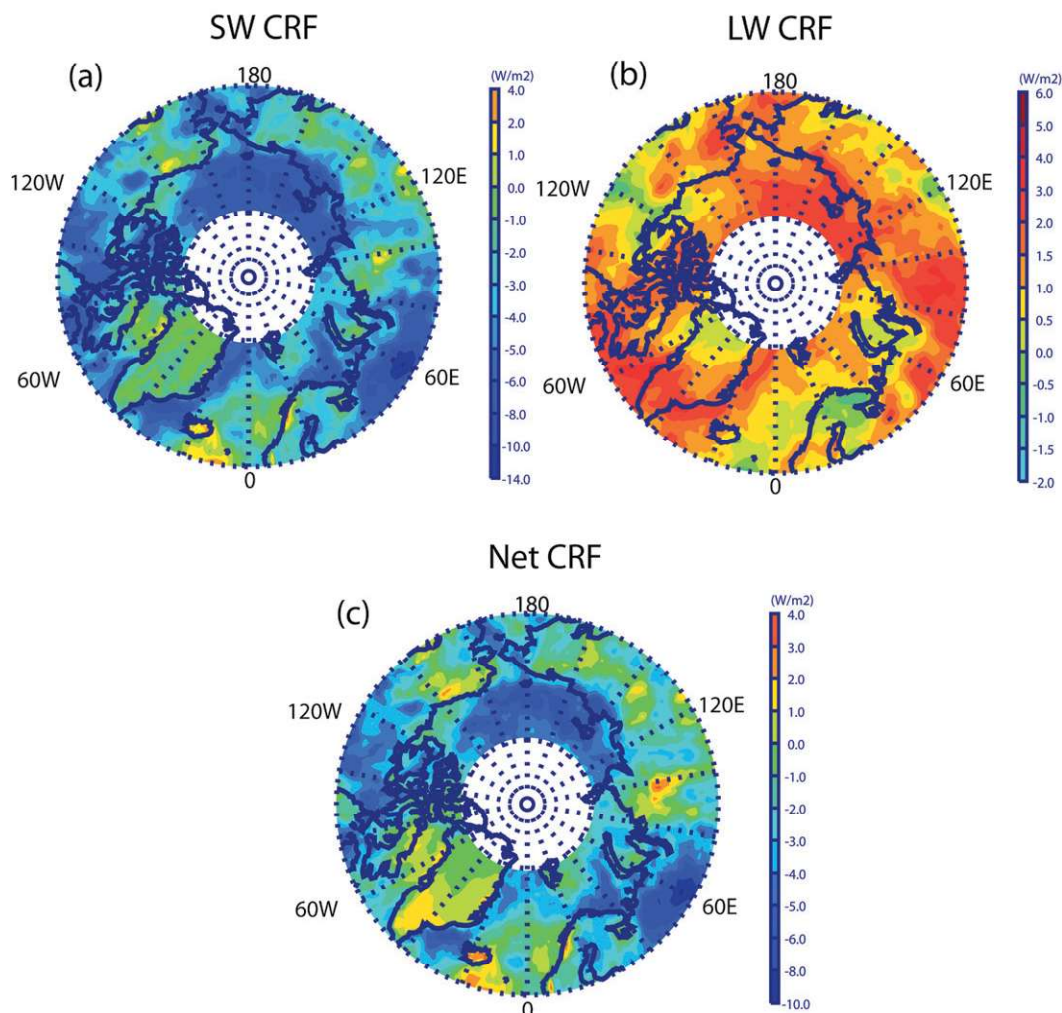


FIG. 9. Polar maps of differences in CRF at the TOA averaged over March–September between CAM5DM and CAM50 for (a) SW CRF, (b) LW CRF, and (c) net CRF.

indicated by Clothiaux et al. (2000), the laser ceilometers and micropulse lidar can provide quite accurate cloud-base measurements.

Even with these issues, the cloud radar and other remote sensors provide valuable information about the vertical distribution of clouds over the ARM Barrow site and are useful for qualitative assessment of climate models (e.g., Qian et al. 2012). As indicated in Fig. 10a, the ARM data show that low-level clouds (below 800 hPa) occur most frequently over the ARM Arctic observational site. This feature is well captured by CAM50. However, CAM50 significantly overestimates the observed clouds at all altitudes for all seasons. The errors in **AU7** CAM50-simulated cloud fraction above are typically

larger than the observed temporal variability in its seasonal mean. The overestimate in the upper troposphere could be partially because cloud radar is not able to detect small cloud particles. Again, this suggests the need for a ground-based radar simulator to improve the model–observation comparison. It is noted that the problem with excessive clouds in the lower troposphere shown in CAM50 is largely reduced in CAM5DM, specifically for the spring, fall, and winter. In the middle and upper troposphere, CAM5DM produces more clouds for all the seasons than CAM50.

Consistent with earlier discussions, CAM5DM simulates more LWP relative to CAM50 except for May and June where both models simulate comparable LWP

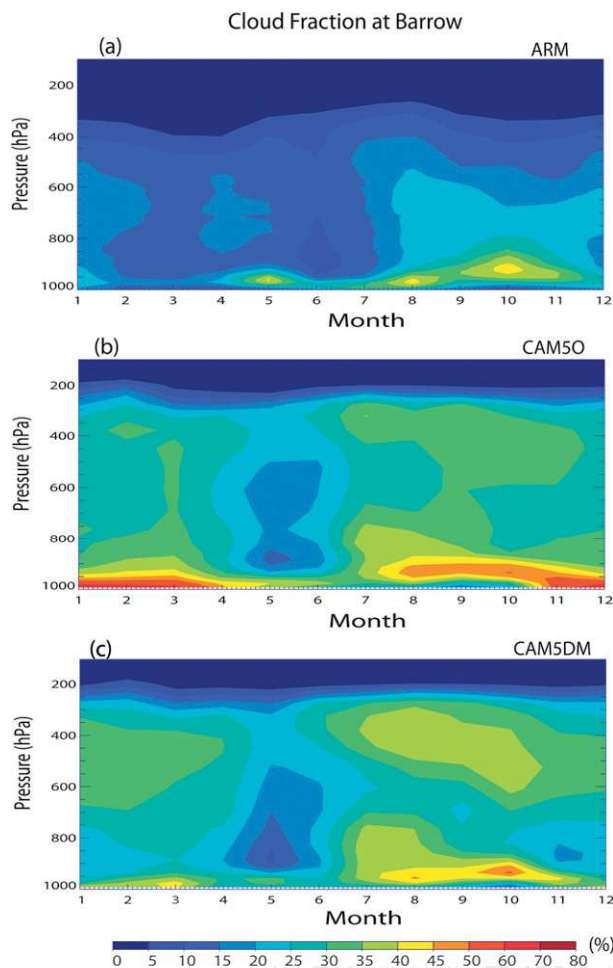


FIG. 10. Monthly-mean cloud fraction from (a) ARM, (b) CAM50, and (c) CAM5DM at Barrow, Alaska.

F12 (Fig. 12a). One long-standing error in CAM-simulated clouds is that they contain very little liquid during the winter months in the Arctic region. This problem is seen in Fig. 12a, which shows that CAM50 has almost zero liquid in its clouds produced from November to March. It is encouraging to see that this error is clearly reduced with the use of the new ice nucleation scheme. Overall, the low LWP bias in CAM50 is considerably reduced in CAM5DM when compared with the ARM data. Nevertheless, the simulated LWP is still too low in CAM5DM during the fall season where low-level mixed-phase clouds usually dominate. Note that the observed LWP was retrieved from the Microwave Radiometer (MWR) measurements using the algorithm described by Turner et al. (2007), which has an uncertainty of 15–25 g m^{-2} . The generally smaller LWP and more clouds produced by both models in comparison with the ARM observations suggest lower liquid water contents contained in the modeled clouds, which is consistent with the results from Liu et al. (2011).

Figure 12b shows the observed and modeled cloud IWP at Barrow. Note that both observed and modeled IWPs include a component due to snow component since the observations cannot separate snow from ice. **AU8** There are two sources for the observed IWP, which are all based on the ARM cloud radar and lidar measurements. One is obtained from the ARM baseline cloud microphysical properties (MICROBASE) value-added product (Dunn et al. 2011). Another one is derived using the algorithm described in Shupe et al. (2005) and Turner (2005) (Shupe–Turner). **AU9** As shown in Zhao et al. (2012), the major differences in IWP between MICROBASE and Shupe–Turner are from their different cloud phase classifications and corresponding different cloud ice boundaries, and different IWP determination methods. MICROBASE determines the cloud phase simply based on temperature (i.e., T). Ice, mixed-phase, and liquid clouds are defined for $T \leq -16^\circ\text{C}$, $-16^\circ < T < 0^\circ\text{C}$, and $T \geq 0^\circ\text{C}$, respectively. Differently, Shupe–Turner uses a much more complicated method to determine cloud phases. This causes some differences in IWP derived from these two methods. In general, the IWP from Shupe–Turner is larger than that from MICROBASE, especially in the spring and fall where the Shupe–Turner data show seasonal maxima. The two peaks are related to ice occurrence in the atmosphere (in any type of clouds), which has seasonal maxima in the spring and fall, with relatively less occurrence in the midwinter (because of slightly fewer total clouds) and summer (because of warmer temperatures) as shown in Shupe (2011, Fig. 2a). A similar annual cycle (i.e., two peaks in the fall and spring, respectively) can be seen in the Surface Heat Budget of the Arctic Ocean (SHEBA) data (Shupe et al. 2005, 2006). Both the Shupe–Turner and MICROBASE datasets show large interannual variability which makes their difference not very significant for most of the months. Relative to the observations, both models largely overestimate the observed IWPs during the summer and winter months although a slight improvement is seen in CAM5DM.

The differences in the cloud properties can impact radiation. Both CAM50 and CAM5DM capture the seasonal variability of downwelling SW and LW radiative fluxes at the surface well, but they overestimate the observed SW during the spring, fall, and winter while they underestimate it in the summer (Fig. 13a). **F13** These errors are typical larger than the standard deviation of the monthly-mean observations. Slight improvements in the simulated radiative fluxes are seen in CAM5DM, particularly in the winter months. These improvements are thought to be related to the increase of LWP during this period in CAM5DM, which contributes to a reduction in SW radiative flux and an increase in LW radiative

Seasonal Mean Cloud Fraction at Barrow

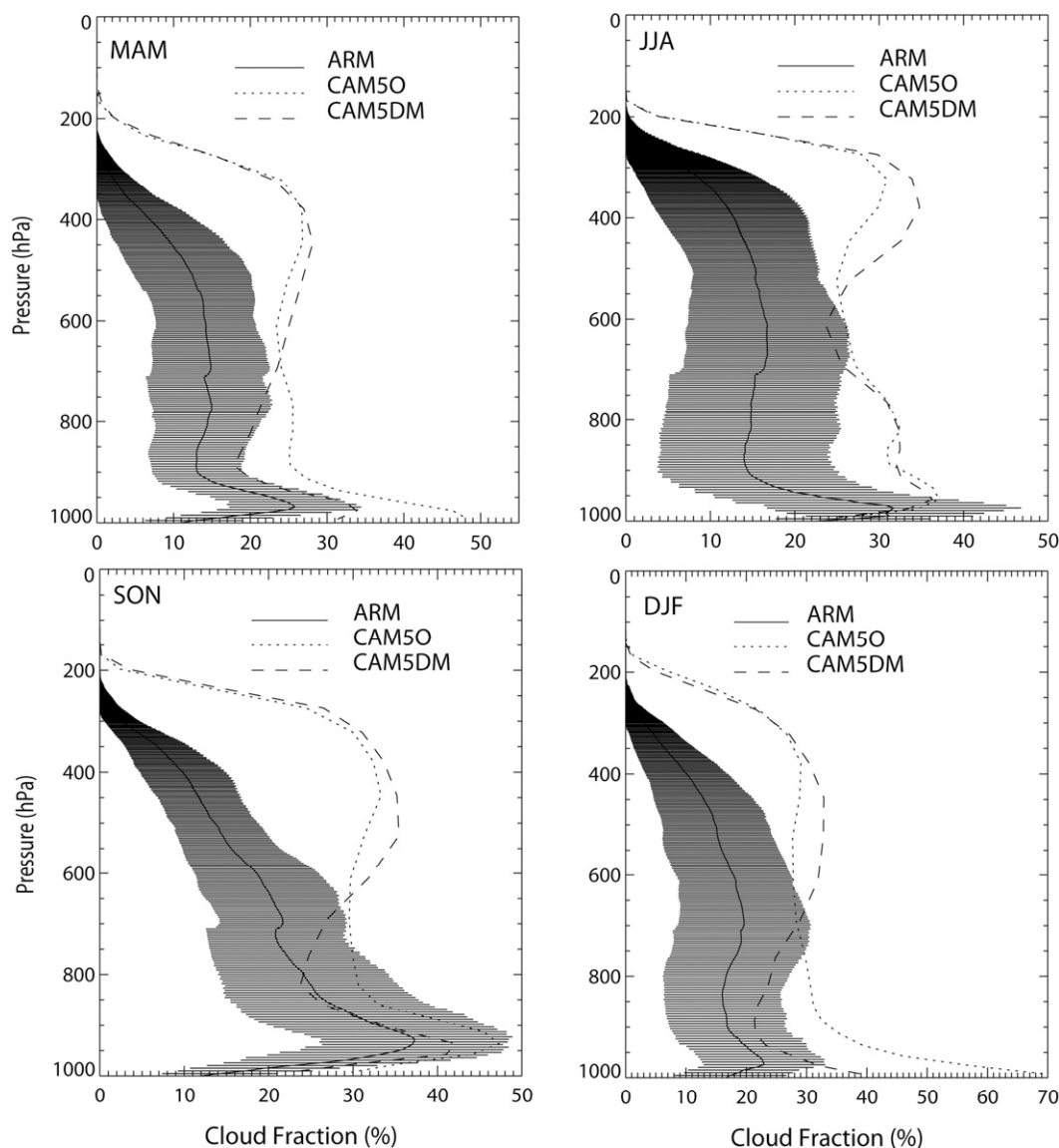


FIG. 11. Vertical profiles of the seasonal-mean observed and modeled cloud fraction. Std dev of the seasonal-mean ARM data are represented by shading.

flux at the surface. However, these changes are minor and are not statistically significant.

4. Summary and discussion

Parameterization of ice nucleation processes in climate models is often based on very limited field studies and therefore has large uncertainties. In this study, we have examined two different ice nucleation schemes with CAM5. One is the scheme developed by M1992, in which the ice number concentration is parameterized as a function of ice supersaturation without considering its

spatial and temporal variations with respect to aerosol properties. This is the default scheme used in CAM5. Another one is the more physically based scheme described in DM2010, which links the variation of ice number concentration to aerosol (dust) particles larger than $0.5 \mu\text{m}$ in diameter in addition to the dependency of temperature. The main purpose is to study the sensitivity of model clouds and radiation to these two different ice nucleation schemes. Model simulations of clouds and radiation are also compared with both satellite and ground-based observations. The focus of the analysis has been in the Arctic region (60° – 80°N).

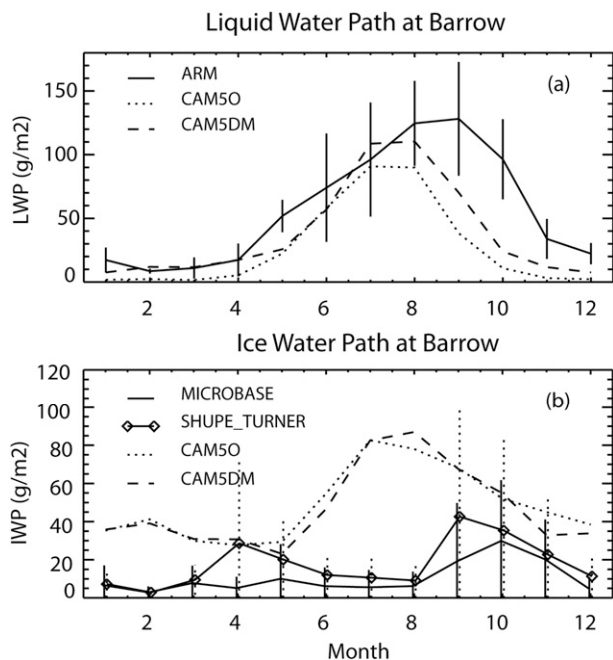


FIG. 12. Monthly-mean observed and modeled (a) LWP and (b) IWP. Error bars indicate std dev of the observed monthly-mean data. In (b), dashed error bars are for std dev in Shupe–Turner and solid error bars are for MICROBASE.

The DM2010 scheme has resulted in a significant reduction (up to two orders of magnitude) of IN concentrations at all latitudes. Changes in cloud amount are mainly seen at high latitudes and the midlatitude storm tracks, where there is a considerable increase in midlevel clouds and a decrease in low-level clouds. The changes in cloud amount result from the complex interaction among cloud macrophysics, microphysics, and the large-scale environment. We have shown that changes in mid- and high-level clouds correspond well with changes in RH while changes in low-level clouds are more related to lower-tropospheric stability. Over these regions, a considerable increase of LWP and decrease of IWP have been found, which are caused by the slowdown of the Bergeron–Findeisen process in mixed-phase clouds caused by the reduction of IN concentrations with the use of DM2010 scheme. There are some inconsistencies regarding the changes in cloud amount and water content, such as the DM2010 scheme, which result in an increase of LWP but a decrease of low-level clouds in the Arctic. This is partly because separate equations are used to determine cloud amount and condensates in CAM5. An effort to consistently treat cloud amount and cloud condensates is currently being made for the future versions of CAM (P. Caldwell, Lawrence Livermore National Laboratory, 2012, personal communication).

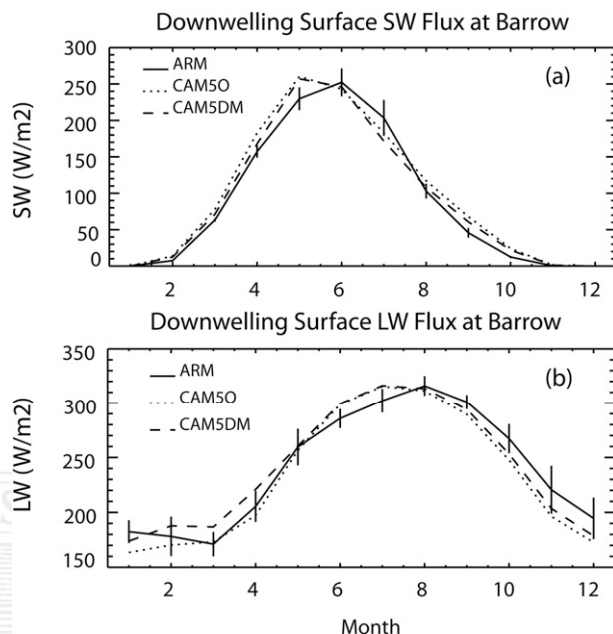


FIG. 13. Monthly-mean observed and modeled downwelling (a) SW radiative fluxes and (b) LW radiative fluxes at the surface. Error bars indicate std dev of the observed monthly-mean data.

The simulated cloud types in the Arctic region are sensitive to the change of the IN concentrations. Relative to the M1992 scheme, the DM2010 scheme has led to a large increase in optically intermediate and thick middle-top clouds and a moderate increase in optically thick high- and low-top clouds. It generally generates fewer optically thin high- and low-top clouds. Overall, the DM2010 scheme has resulted in an increase of optical depth of Arctic clouds and made Arctic clouds brighter. As a result, DM2010 has led to a stronger SW, LW, and net cloud radiative forcing (cooling) at the TOA.

Differences are often seen in different satellite datasets because of considerable differences in the algorithms used to retrieve cloud and radiation properties from satellite measurements. Despite these differences, it appears that the DM2010 scheme slightly improves the model simulation of optically thin low-level clouds, while it exaggerates the problem that the model produces too many optically thick mid- and high-level clouds when compared with both the ISCCP and MODIS observations in the Arctic. A comparison with CALIPSO clouds indicates that the default CAM5 overproduces the Arctic clouds in all altitudes, especially at low levels. The new IN scheme leads to a slight reduction in the low-level cloud amount over most of the Arctic, while it exaggerates the biases in midlevel clouds.

The ARM long-term ground-based measurements at its Barrow site are also used to evaluate CAM5 cloud

and radiation simulations. It has been seen that CAM5 with the DM2010 scheme produces clearly better results in simulating low-level clouds and their properties relative to the ARM data. The increased LWP in CAM5DM, particularly during the winter months, is very encouraging because CAM-simulated cold clouds often contain very little liquid. The better-simulated clouds lead to slightly better simulations in surface SW and LW radiative fluxes; however, these improvements are not statistically significant.

Results from this study indicate the importance of a better representation of ice nucleation process in mixed-phase clouds in climate models, especially for high latitudes where mixed-phase clouds are one dominant cloud type. Linking ice nucleation parameterization to aerosol properties allows climate models to better represent aerosol–cloud coupling and aerosol indirect forcing. Recent studies have investigated the aerosol impact on pure ice (cirrus) clouds through homogeneous and heterogeneous ice nucleation with various ice nucleation schemes in CAM5 (Gettelman et al. 2012; Liu et al. 2012a). Gettelman et al. (2012) showed that the indirect effect of anthropogenic aerosols on cirrus clouds can be around $0.27 \pm 0.1 \text{ W m}^{-2}$ (1σ uncertainty), which occurs as a result of increasing homogeneous nucleation of anthropogenic sulfate in CAM5. Liu et al. (2012a) indicated that dust ice nuclei can change the present-day net cloud forcing of cirrus clouds by $-0.24 \pm 0.28 \text{ W m}^{-2}$ to $-0.40 \pm 0.20 \text{ W m}^{-2}$ in CAM5 because of its inhabitation of homogenous nucleation of sulfate with different formulations of heterogeneous dust ice nucleation.

We note that the dependence on aerosol properties of ice nucleation parameterizations requires more accurate simulations of aerosol fields in the climate models. Like most climate models, CAM5 has a low bias in its predicted aerosol concentrations in the Arctic because of the too fast wet removal of aerosols during their transport from midlatitudes (Liu et al. 2012b). The low aerosol concentration bias can result in a low bias in cloud droplet and ice crystal number concentrations. This increases the droplet size and accelerates the autoconversion from cloud liquid water to rainwater and thus leads to a low cloud liquid water bias in CAM5 (Liu et al. 2011). On the other hand, the lower ice crystal number will result in a slower conversion from cloud liquid to ice by the Bergeron–Findeisen process. The net effect on cloud water content will be investigated in a future study. Recent studies (e.g., Wang et al. 2012, manuscript submitted to *J. Geophys. Res.*) have shown that improved representations of aerosol (e.g., for aerosol transport and removal of aerosols in convective clouds) and cloud micro- and macrophysics have significantly improved the aerosol simulations, especially at high

latitudes. More robust evaluations of these physically based ice nucleation schemes could be done with improved aerosol simulations and observations in the future.

Acknowledgments. S. Xie, C. Zhao, and Y. Zhang are supported by the Earth System Modeling Program and Atmospheric Radiation Measurement Program of the Office of Science at the U.S. Department of Energy (DOE). Support for X. Liu was provided by the DOE Office of Science Atmospheric System Research (ASR) Program and Earth System Modeling Program. Work at LLNL was performed under the auspices of the DOE, Office of Science, Office of Biological and Environmental Research by Lawrence Livermore National Laboratory under Contract DE-AC52-07NA27344. The Pacific Northwest National Laboratory (PNNL) is operated for the DOE by Battelle Memorial Institute under Contract DE-AC06-76RLO 1830. Discussions with Neil Barton, Stephen Klein, James Boyle, and Yunyan Zhang of Lawrence Livermore National Laboratory were helpful. We also thank the anonymous reviewers, whose valuable comments helped to clarify and improve the paper.

REFERENCES

- Al-Naimi, R., and C. P. R. Saunders, 1985: Measurements of natural deposition and condensation-freezing ice nuclei with a continuous flow chamber. *Atmos. Environ.*, **19**, 1871–1882.
- Barkstrom, B., 1984: The Earth Radiation Budget Experiment. *Bull. Amer. Meteor. Soc.*, **65**, 1170–1185.
- Barton, N. P., S. A. Klein, J. S. Boyle, and Y. Y. Zhang, 2012: Arctic synoptic regimes: Comparing domain-wide Arctic cloud observations with CAM4 and CAM5 during similar dynamics. *J. Geophys. Res.*, **117**, D15205, doi:10.1029/2012JD017589.
- Bergeron, T., 1935: On the physics of clouds and precipitation. *Proces Verbaux de l'Association de Meteorologie*, International Union of Geodesy and Geophysics, 156–178.
- Bigg, E. K., 1996: Ice forming nuclei in the high Arctic. *Tellus*, **48**, 223–233.
- Bodas-Salcedo, A., and Coauthors, 2011: COSP: Satellite simulation software for model assessment. *Bull. Amer. Meteor. Soc.*, **92**, 1023–1043.
- Bony, S., M. Webb, C. Bretherton, S. A. Klein, P. Siebesma, G. Tselioudis, and M. Zhang, 2011: CFMIP: Towards a better evaluation and understanding of clouds and cloud feedbacks in CMIP5 models. *CLIVAR Exchanges*, No. 56, International CLIVAR Project Office, Southampton, United Kingdom, 20–24.
- Chen, J.-P., A. Hazra, and Z. Levin, 2008: Parameterizing ice nucleation rates using contact angle and activation energy derived from laboratory data. *Atmos. Chem. Phys.*, **8**, 7431–7449.
- Chepfer, H., S. Bony, D. Winker, G. Cesana, J. L. Dufresne, P. Minnis, C. J. Stubenrauch, and S. Zeng, 2010: The GCM-Oriented CALIPSO Cloud Product (CALIPSO-GOCCP). *J. Geophys. Res.*, **115**, D00H16, doi:10.1029/2009JD012251.
- Clothiaux, E. E., T. P. Ackerman, G. G. Mace, K. P. Moran, R. T. Marchand, M. A. Miller, and B. E. Martner, 2000: Objective determination of cloud heights and radar reflectivities using

- a combination of active remote sensors at the ARM CART sites. *J. Appl. Meteor.*, **39**, 645–665.
- DeMott, P. J., and Coauthors, 2010: Predicting global atmospheric ice nuclei distributions and their impacts on climate. *Proc. Natl. Acad. Sci. USA*, **107**, 11 217–11 222, doi:10.1073/pnas.0910818107.
- Diehl, K., C. Quick, S. Matthias-Maser, S. K. Mitra, and R. Jaenicke, 2001: The ice nucleating ability of pollen. Part I: Laboratory studies in deposition and condensation freezing modes. *Atmos. Res.*, **58**, 75–87.
- Dunn, M., K. L. Johnson, and M. P. Jensen, 2011: The Microbase value-added product: A baseline retrieval of cloud microphysical properties. U.S. Department of Energy Office of Science Rep. DOE/SC-ARM/TR-095, 34 pp. [Available online at http://www.arm.gov/publications/tech_reports/doe-scp-arm-tr-095.pdf.]
- Ekman, A. M. L., A. Engstrom, and C. Wang, 2007: The effect of aerosol composition and concentration on the development and anvil properties of a continental deep convective cloud. *Quart. J. Roy. Meteor. Soc.*, **133**, 1439–1452.
- Findeisen, W., 1938: Kolloid-meteorologische Vorgänge bei Neiderschlags-bildung. *Meteor. Z.*, **55**, 121–133.
- Gates, W. L., and Coauthors, 1999: An overview of the results of the Atmospheric Model Intercomparison Project (AMIP I). *Bull. Amer. Meteor. Soc.*, **80**, 29–55.
- Gettelman, A., X. Liu, S. J. Ghan, H. Morrison, S. Park, and A. J. Conley, 2010: Global simulations of ice nucleation and ice supersaturation with an improved cloud scheme in the Community Atmospheric Model. *J. Geophys. Res.*, **115**, D18216, doi:10.1029/2009JD013797.
- , —, D. Barahona, U. Lohmann, and C. Chen, 2012: Climate impacts of ice nucleation. *J. Geophys. Res.*, **117**, D20201, doi:10.1029/2012JD017950.
- Gorbunov, B., A. Baklanov, N. Kakutkina, H. L. Windsor, and R. Toumi, 2001: Ice nucleation on soot particles. *J. Aerosol Sci.*, **32**, 199–215.
- Hassol, S. J., 2004: *Impacts of a Warming Arctic: Arctic Climate Impact Assessment*. Cambridge University Press, 1020 pp.
- Karcher, B., and U. Lohmann, 2003: A parameterization of cirrus cloud formation: Heterogeneous freezing. *J. Geophys. Res.*, **108**, 4402, doi:10.1029/2002JD003220.
- Kay, J. E., M. M. Holland, and A. Jahn, 2011a: Inter-annual to multi-decadal Arctic sea ice extent trends in a warming world. *Geophys. Res. Lett.*, **38**, L15708, doi:10.1029/2011GL048008.
- , K. Raeder, A. Gettelman, and J. Anderson, 2011b: The boundary layer response to recent Arctic sea ice loss and implications for high-latitude climate feedbacks. *J. Climate*, **24**, 428–447.
- , M. M. Holland, C. M. Bitz, E. Blanchard-Wrigglesworth, A. Gettelman, A. Conley, and D. Bailey, 2012a: The influence of local feedbacks and northward heat transport on the equilibrium Arctic climate response to increased greenhouse gas forcing. *J. Climate*, **25**, 5433–5450.
- , and Coauthors, 2012b: Exposing global cloud biases in the Community Atmosphere Model (CAM) using satellite observations and their corresponding instrument simulators. *J. Climate*, **25**, 5190–5207.
- Klein, S. A., and D. L. Hartmann, 1993: The seasonal cycle of low stratiform clouds. *J. Climate*, **6**, 1587–1606.
- Levin, Z., and S. A. Yankofsky, 1983: Contact versus immersion freezing of freely suspended droplets by bacterial ice nuclei. *J. Climate Appl. Meteor.*, **22**, 1964–1966.
- Liu, X., J. E. Penner, S. Ghan, and M. Wang, 2007a: Inclusion of ice microphysics in the NCAR Community Atmospheric Model version 3 (CAM3). *J. Climate*, **20**, 4526–4547.
- , S. Xie, and S. J. Ghan, 2007b: Evaluation of a new mixed-phase cloud microphysics parameterization with CAM3 single-column model and M-PACE observations. *Geophys. Res. Lett.*, **34**, L23712, doi:10.1029/2007GL031446.
- , and Coauthors, 2011: Testing cloud microphysics parameterizations in NCAR CAM5 with ISDAC and M-PACE observations. *J. Geophys. Res.*, **116**, D00T11, doi:10.1029/2011JD015889.
- , X. Shi, K. Zhang, E. J. Jensen, A. Gettelman, D. Barahona, A. Nenes, and P. Lawson, 2012a: Sensitivity studies of dust ice nuclei effect on cirrus clouds with the Community Atmosphere Model CAM5. *Atmos. Chem. Phys.*, **12**, 12 061–12 079, doi:10.5194/acp-12-12061-2012.
- , and Coauthors, 2012b: Toward a minimal representation of aerosols in climate models: Description and evaluation in the Community Atmosphere Model CAM5. *Geosci. Model Dev.*, **5**, 709–739, doi:10.5194/gmd-5-709-2012.
- Loeb, N. G., B. A. Wielicki, D. R. Doelling, G. L. Smith, D. F. Keyes, S. Kato, N. Manalo-Smith, and T. Wong, 2009: Towards optimal closure of the Earth's top-of-atmosphere radiation budget. *J. Climate*, **22**, 748–766.
- Meyers, M. P., P. J. DeMott, and W. R. Cotton, 1992: New primary ice nucleation parameterizations in an explicit cloud model. *J. Appl. Meteor.*, **31**, 708–721.
- Morrison, H., and A. Gettelman, 2008: A new two-moment bulk stratiform cloud microphysics scheme in the NCAR Community Atmosphere Model (CAM3). Part I: Description and numerical tests. *J. Climate*, **21**, 3642–3659.
- , G. de Boer, G. Feingold, J. Harrington, M. Shupe, and K. Sulia, 2012: Resilience of persistent Arctic mixed-phase clouds. *Nat. Geosci.*, **5**, 11–17, doi:10.1038/ngeo1332.
- Neale, R. B., J. H. Richter, and M. Jochum, 2008: The impact of convection on ENSO: From a delayed oscillator to a series of events. *J. Climate*, **21**, 5904–5924.
- Niemand, M., and Coauthors, 2012: A particle-surface-area-based parameterization of immersion freezing on desert dust particles. *J. Atmos. Sci.*, **69**, 3077–3092.
- Phillips, V. T. J., and Coauthors, 2005: Anvil glaciation in a deep cumulus updraft over Florida simulated with an Explicit Microphysics Model. I: The impact of various nucleation processes. *Quart. J. Roy. Meteor. Soc.*, **131**, 2019–2046.
- , P. J. DeMott, and C. Andronache, 2008: An empirical parameterization of heterogeneous ice nucleation for multiple chemical species of aerosol. *J. Atmos. Sci.*, **65**, 2757–2783.
- Pincus, R., S. Platnick, S. A. Ackerman, R. S. Hemler, and R. J. P. Hoffmann, 2012: Reconciling simulated and observed views of clouds: MODIS, ISCCP, and the limits of instrument simulators. *J. Climate*, **25**, 4699–4720.
- Platnick, S., M. D. King, S. A. Ackerman, W. P. Menzel, B. A. Baum, J. C. Riedi, and R. A. Frey, 2003: The MODIS cloud products: Algorithms and examples from Terra. *IEEE Trans. Geosci. Remote Sens.*, **41**, 459–473, doi:10.1109/TGRS.2002.808301.
- Prenni, A. J., and Coauthors, 2007: Can ice-nucleating aerosols affect Arctic seasonal climate? *Bull. Amer. Meteor. Soc.*, **88**, 541–550.
- Qian, Y., C. N. Long, H. Wang, J. M. Comstock, S. A. McFarlane, and S. Xie, 2012: Evaluation of cloud fraction and its radiative effect simulated by IPCC AR4 global models against ARM surface observations. *Atmos. Chem. Phys.*, **12**, 1785–1810, doi:10.5194/acp-12-1785-2012.
- Rasch, P. J., and J. E. Kristjánsson, 1998: A comparison of the CCM3 model climate using diagnosed and predicted condensate parameterizations. *J. Climate*, **11**, 1587–1614.

- Rogers, D. C., 1982: Field and laboratory studies of ice nucleation in winter orographic clouds. Ph. D. dissertation, University of Wyoming, 161 pp.
- Rossow, W. B., and R. A. Schiffer, 1999: Advances in understanding clouds from ISCCP. *Bull. Amer. Meteor. Soc.*, **80**, 2261–2288.
- Shupe, M. D., 2011: Clouds at Arctic atmospheric observatories. Part II: Thermodynamic phase characteristics. *J. Appl. Meteor. Climatol.*, **50**, 645–661.
- , T. Uttal, and S. Y. Matrosov, 2005: Arctic cloud microphysics retrievals from surface-based remote sensors at SHEBA. *J. Appl. Meteor.*, **44**, 1544–1562.
- , S. Y. Matrosov, and T. Uttal, 2006: Arctic mixed-phase cloud properties derived from surface-based sensors at SHEBA. *J. Atmos. Sci.*, **63**, 697–711.
- Turner, D. D., 2005: Arctic mixed-phase cloud properties from AERI lidar observations: Algorithm and results from SHEBA. *J. Appl. Meteor.*, **44**, 427–444.
- , S. A. Clough, J. C. Liljegren, E. E. Clothiaux, K. Cady-Pereira, and K. L. Gaustad, 2007: Retrieving liquid water path and precipitable water vapor from Atmospheric Radiation Measurement (ARM) microwave radiometers. *IEEE Trans. Geosci. Remote Sens.*, **45**, 3680–3690.
- Vavrus, S., D. Waliser, A. Schweiger, and J. Francis, 2009: Simulations of 20th and 21st century Arctic cloud amount in the global climate models assessed in the IPCC AR4. *Climate Dyn.*, **33**, 1099–1115.
- Verlinde, J., and Coauthors, 2007: The Mixed-Phase Arctic Cloud Experiment. *Bull. Amer. Meteor. Soc.*, **88**, 205–221.
- Walsh, J. E., V. M. Kattsov, W. L. Chapman, V. Govorkova, and T. Pavlova, 2002: Comparison of Arctic climate simulations by uncoupled and coupled global models. *J. Climate*, **15**, 1429–1446.
- Wang, H., and Coauthors, 2012: Improving aerosol transport to high-latitudes in CAM5. *J. Geophys. Res.*, submitted. **AU10**
- Wielicki, B. A., B. R. Barkstorm, E. F. Harrison, R. B. Lee III, G. L. Smith, and J. E. Cooper, 1996: Clouds and the Earth's Radiant Energy System (CERES): An Earth Observing System experiment. *Bull. Amer. Meteor. Soc.*, **77**, 853–868.
- Winton, M., 2006: Amplified Arctic climate change: What does surface albedo feedback have to do with it? *Geophys. Res. Lett.*, **33**, L03701, doi:10.1029/2005GL025244.
- Xie, S., J. Boyle, S. A. Klein, X. Liu, and S. Ghan, 2008: Simulations of Arctic Mixed-Phase Clouds in Forecasts with CAM3 and AM2 for M-PACE. *J. Geophys. Res.*, **113**, D04211, doi:10.1029/2007JD009225.
- , and Coauthors, 2010: Clouds and more: ARM climate modeling best estimate data. *Bull. Amer. Meteor. Soc.*, **91**, 13–20.
- Zender, C., H. Bian, and D. Newman, 2003: Mineral Dust Entrainment and Deposition (DEAD) model: Description and 1990s dust climatology. *J. Geophys. Res.*, **108**, 4416, doi:10.1029/2002JD002775.
- Zeng, X., W.-K. Tao, M. Zhang, A. Y. Hou, S. Xie, S. Lang, X. Li, D. Starr, and X. Li, 2009: A contribution by ice nuclei to global warming. *Quart. J. Roy. Meteor. Soc.*, **135**, 1614–162.
- Zhang, G. J., and N. A. McFarlane, 1995: Sensitivity of climate simulations to the parameterization of cumulus convection in the Canadian Climate Center general circulation model. *Atmos.–Ocean*, **33**, 407–446.
- Zhang, Y., B. Stevens, B. Medeiros, and M. Ghil, 2009: Low-cloud fraction, lower-tropospheric stability, and large-scale divergence. *J. Climate*, **22**, 4827–4844.
- Zhao, C., and Coauthors, 2012: Toward understanding of differences in current cloud retrievals of ARM ground-based measurements. *J. Geophys. Res.*, **117**, D10206, doi:10.1029/2011JD016792.

